Supercritical Hydrothermal Synthesis of Lithium Iron Phosphate ($LiFePO_4$) Nanoparticles

Seung-Ah Hong[1,2], Jaehoon Kim[1*], Jae-Duck Kim[1], Youn-Woo Lee[2], Jeong Won Kang[3]

[1]Supercritical Fluid Research Laboratory, Energy and Environment Research Division,
Korea Institute of Science and Technology (KIST)
39-1 Hawolgok-dong Seoungbuk-gu, 136-791, Seoul, Korea

[2]School of Chemical and Biological Engineering, Seoul National University,
Gwanangro 599, Gwanak-gu, Seoul 151-744, Korea

[3]Department of Chemical & Biological Engineering, Korea University,
5-1 Anam Dong, Sungbuk-Ku, Seoul 136-701, Korea

*Corresponding author: Tel: +82-2-958-5873, E-mail; Jaehoonkim@kist.re.kr, Fax: 82-2-958-5205

ABSRACT

Lithium iron phosphate ($LiFePO_4$) was synthesized using supercritical hydrothermal synthesis in a continuous mode. The effects of precursor solution concentration, water flow rate, and temperature on the particle size and crystallinity were examined using scanning electron microscopy (SEM), X-ray diffraction (XRD), Brunauer, Emmet, and Teller (BET) surface area analysis. Cycling performance of the particles was examined using charge/discharge testing. An initial discharge capacity of 130 mAh/g and 110 mAh/g after 35 cycles resulted.

INTRODUCTION

Lithium iron phosphate ($LiFePO_4$) has been attracted much attention as a promising cathode active material due to its valuable physical and electrochemical properties. This includes high stability at elevated temperature, safety under abusive conditions, good energy density, low cost of the starting materials, and lack of toxicity. These valuable properties of $LiFePO_4$ make it suitable for large-scale applications such as hybrid electric vehicles (HEV) or plug in hybrid electric vehicle (PHEV). Various synthetic methods were developed including solid-state method [1,2,3], spray pyrolysis method [4], hydrothermal method [5,6,7], co-precipitation method [8,9], sol-gel method [3,10]. These methods often suffer from long production time, generation of large organic or aqueous waste, high synthesis temperature, low production rate associated with batch mode operation. Supercritical hydrothermal

synthesis (SHS) is a very promising method to produce high-quality, highly crystalline, and nanosize metal oxide particles. In addition, supercritical hydrothermal synthesis (SHS) is an environmental-friendly, fast and continuous method and readily scalable. Herein we studied synthesis of $LiFePO_4$ using a continuous supercritical hydrothermal method. The effects of precursor solution concentration, temperature, flow rate were examined in detail. The electrochemical performance was also examined.

MATERRIALS AND METHOD

Nitrogen (purity of 99.9 %) was purchased from Shinyang Sanso Co. (Seoul, Korea). Distilled and deionized (DDI) water was prepared using a Milli-Q, Ultrapure water purification system with a 0.22 μm filter (Billerica, MA). Lithium hydroxide monohydrate ($LiOH{\cdot}H_2O$, purity of > 98 wt %), iron sulfate heptahydrate ($FeSO_4{\cdot}7\ H_2O$, purity of > 99 wt %), phosphoric acid (H_3PO_4, purity of > 98 wt %) were purchased by Sigma-Aldrich (St. Louis, MO). Mixed cellulose ester membrane filter with a pore size of 0.45 μm was purchased from Toyo Roshi Kaisha Ltd. (Tokyo, Japan).

All synthesis experiment was carried out with continuous supercritical hydrothermal synthesis (SHS). Details on the extraction apparatus are given in the previous paper [11].

Prior to each experiment, the precursor solutions and the DDI were purged with nitrogen at least 1 hour to reduce the amount of dissolved oxygen and to prevent oxidation from Fe^{2+} to Fe^{3+}. The DDI water was then introduced into the reactor system using the high-pressure pumps at an experimentally desired pressure of 250 bar. The pressure of the reactor was controlled by the back-pressure regulator. The temperatures of the reactor and the pre-heater were then increased to an experimentally desired temperature of 400 ºC using two heat furnaces. After experimentally desired temperature and pressure was reached, the precursor solutions were introduced into the reactor system. Typically, the temperature of the reactor and the mixing tee can be maintained at 400 ± 5 °C over the length of the reactor and the pressure can be maintained at 250 ± 1 bar over the entire reaction time. After a desired period of synthesis, the DDI water was passed through the reactor at least 30 min. The temperature of the reactor was then decreased to room temperature and the synthesized particles in the metal filters were collected. The particles were then rinsed with DDI water and filtered using the mixed cellulose ester membrane filter.

After washing the particles in metal filter, and then they were weighed and analyzed. The morphology of the particles was observed using A Hitachi S-4100 (NY, USA) field emission scanning electron microscope (FE-SEM). The structure of the particles were characterized by X-ray diffraction (XRD) using a D/Max-2500 Rigaku X-ray diffractometer (Rigaku, Japan) with a Cu Kα excitation source (λ = 1.5405 □) using 30 KV at 35 mA. The surface area of the particles was measured using a Belsorp-max mini □ apparatus (BEL Inc., Japan).

RESULTS

Various synthesis conditions including temperature, flow rates, concentration were examined and the results are shown in Table 1. The pressure was fixed at 250 bar, the flow rate ratio of the reactants ($FeSO_4 \cdot H_3PO_4$:LiOH:H_2O) was fixed to 1.5:1.5:25 and the feed concentration ratio of the reactants ($FeSO_4$:H_3PO_4:LiOH) was fixed to 0.01:0.01:0.03.

Table 1 : Summary of synthesis conditions for $LiFePO_4$

Sample No.	Temp. [°C]	Feed Concentration [M]			Flow Rate Ratio [g min^{-1}]			τ [g min^{-1}]	BET Surface Area [m^2 g^{-1}]
		$FeSO_4$	H_3PO_4	LiOH	$FeSO_4 \cdot H_3PO_4$	LiOH	H_2O		
L1	300	0.01	0.01	0.03	1.5	1.5	25	72	11.8
L2	400	0.01	0.01	0.03	1.5	1.5	25	15	17.5
L3	400	0.01	0.01	0.03	3.0	3.0	18	17	10.6
L4	400	0.03	0.03	0.09	3.0	3.0	18	18	12.2
L5	400	0.06	0.06	0.18	3.0	3.0	18	17	17.2
L6	400	0.03	0.03	0.09	1.5	1.5	9	36	7.0
L7	400	0.03	0.03	0.09	1.5	1.5	18	14	13.7
L8	400	0.03	0.03	0.09	1.5	1.5	36	10	24.8
L9	400	0.03	0.03	0.09	1.5	1.5	36	28	21.7

Figure 1 shows the effects of temperature on particle size and crystallinity of $LiFePO_4$. BET surface areas of the samples are listed in Table 1. $LiFePO_4$ synthesized at 300 °C (subcritical water state, L1) retained larger particles with very broad size distribution and smaller BET surface area compared with $LiFePO_4$ synthesized at 400 °C (supercritical water state, L2). Lower solubility of the reactants in supercritical water leads to higher supersaturation compared to those in subcritical water [12-14]. As a result, smaller particles may form in supercritical water. As shown in Figure 1, crystallinity of $LiFePO_4$ synthesized 300 °C is lower than that of $LiFePO_4$ synthesized 400 °C. Smaller particles with higher crystallinity were obtained at supercritical water state. XRD patterns of $LiFePO_4$ synthesized using solid-state method is shown in Figure 1 for comparison. It can be seen that impurities such as $FeH_3(PO_3) \cdot 2H_2O$, $Fe(PO_3)_3$ were observed in the particles synthesized at 400 °C.

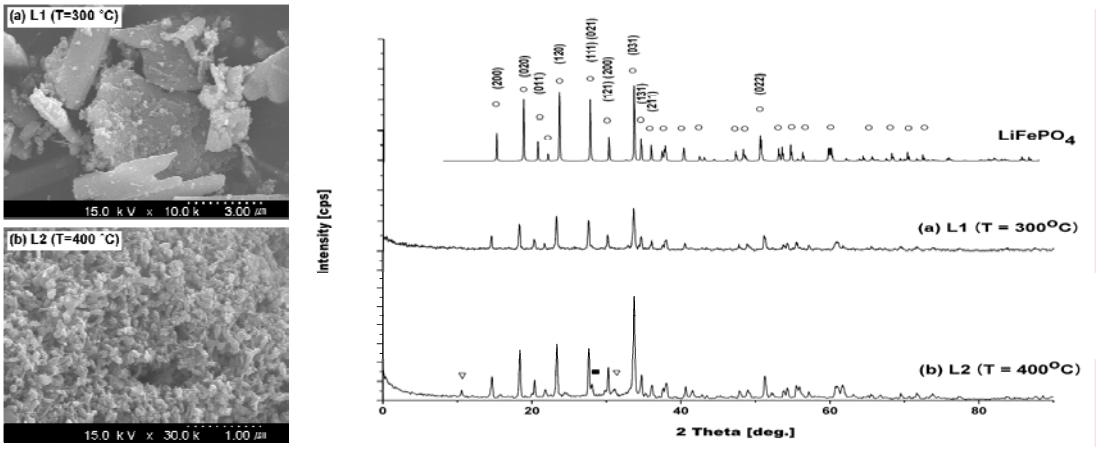

Figure 1 : SEM images of (a) L1, , (b) L2. XRD patterns of $LiFePO_4$ synthesized using solid-state method, (a) L1, (b) L2 (○; $LiFePO_4$, □ ; $LiFeH_4(P_2O_7)_2$, △; β-Fe_2O_3, ▽;$FeH_3(PO_3)\cdot 2H_2O$, ▲; $FePO_4H_2O$, ■;$Fe(PO_3)_3$, ▼; Li_3PO_4)

The effect of precursor concentrations on the particle size and crystallinity were examined and the results are shown in Figure 2. The temperature was fixed to 400 °C, the pressure was fixed to 250 bar and flow rate ratio of $FeSO_4\cdot H_3PO_4$:LiOH:H_2O was fixed at 3:3:18 (see Table 1). The particles synthesized at the higher precursor concentration are smaller and BET surface area is larger compared to those of the particles synthesized at lower concentration. Higher supersaturation ratio at higher concentration can result in smaller particle size.

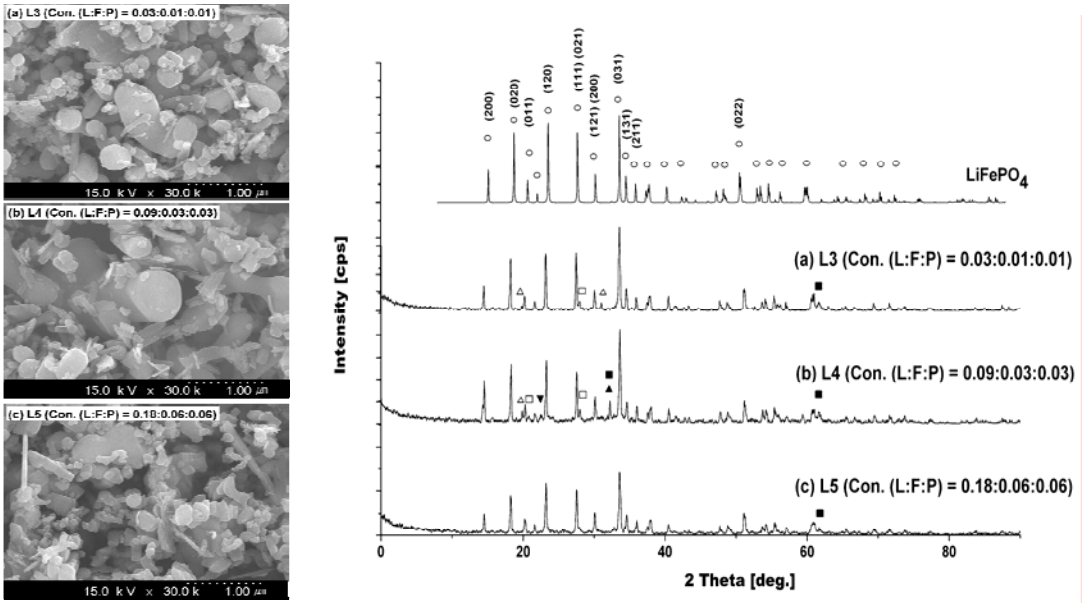

Figure 2 : SEM images of L3, (b) L4, and (c) L5. XRD patterns of $LiFePO_4$ synthesized by solid-state method, (a) L3, (b) L4, (c) L5 (○; $LiFePO_4$, □ ; $LiFeH_4(P_2O_7)_2$, △; β-Fe_2O_3, ▽;$FeH_3(PO_3)\cdot 2H_2O$, ▲; $FePO_4H_2O$, ■;$Fe(PO_3)_3$, ▼; Li_3PO_4)

As shown in Figure 2, crystallinity of the particles synthesized at various concentrations did not change much.

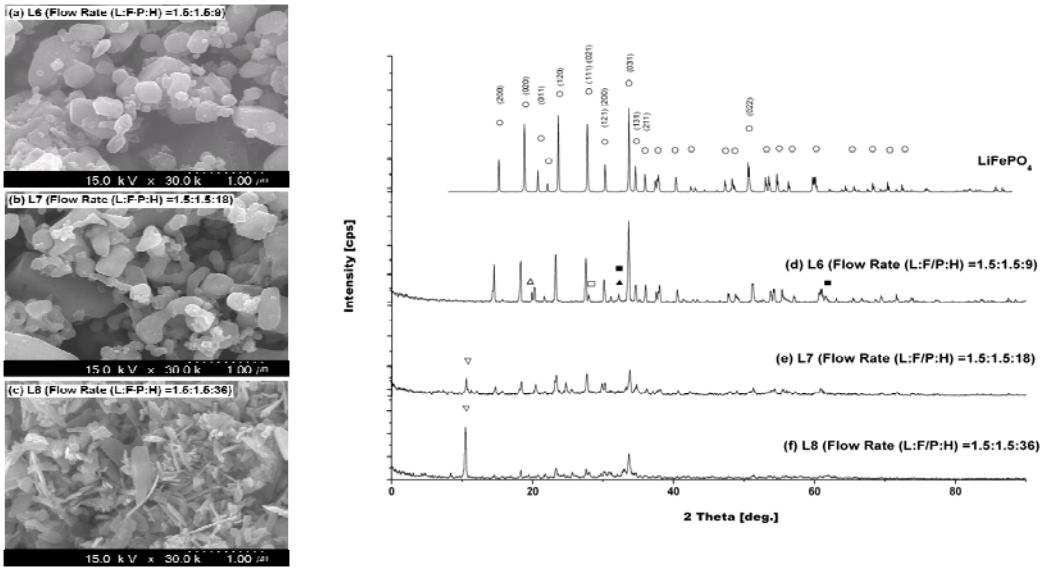

Figure 3 : SEM images of (a) L6 (b) L7 (c) L8. XRD patterns of $LiFePO_4$ synthesized using solid-state method, (d) L6, (e) L7, (f) L8 (○; $LiFePO_4$, □ ; $LiFeH_4(P_2O_7)_2$, △; β-Fe_2O_3, ▽;$FeH_3(PO_3)\cdot 2H_2O$, ▲; $FePO_4H_2O$, ■;$Fe(PO_3)_3$, ▼; Li_3PO_4)

The effect of water flow rates on the particle size and the crystallinity were examined and the results are shown in Figure 3. As the water flow rate increased from 9 g/min to 36 g/min, the BET surface area significantly decreased from 7.0 to 24.8 m^2/g, suggesting that the particle size decreased at higher water flow rate. As shown in Figure 3, the particles synthesized at 36 g/min retained needle-like morphology. However, the crystallinity of the particles synthesized at higher flow rate decreased significantly.

Electro performance of the L4 and L6 are shown in Figure 4. The charge/discharge capacity of sample L6 raw $LiFePO_4$ is about 90 mAh/g at 0.1 C rate. All the curves show a good cycling stability at cycle life than $LiFePO_4$ was synthesized by solid-state [15]. Sample L4 with coating carbon were improved the electro performance from 80 to 120 mAh/g. Thus LiFePO4 synthesized with the supercritical hydrothermal synthesis can be suitable for active cathode materials of large-scale lithium ion batteries.

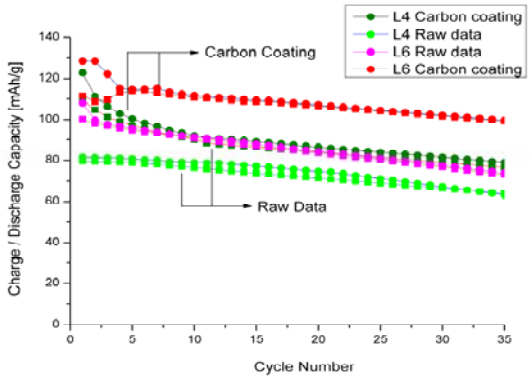

Figure 4 : Electro performances of L4 and L6

CONCLUSION

Complete synthesized $LiFePO_4$ using a continuous SHS technique takes a short time due to its relatively high diffusivity and solubility in SCW. Our results show that particle size and crystallinity can be controlled by adjusting temperature, concentration and water flow rate. An initial discharge capacity of 130 mAh/g and 110 mAh/g after 35 cycles resulted.

REFERANCES

[1] John O. Thomas, A. S. A., Beata Kalska , Lennart Haggstrom (2000). Solid State Ionics 130: 41-52.

[2] U. Amador, O. G. a.-M., M. Alvarez-Vega, F. Garcı´a-Alvarado, J. Garcı´a-Jaca, J. M. Gallardo-Amores, M. L. Sanjua´n (2001). Chemistry of materials 13: 1570-1576.

[3] L. F. Nazar , B. E., M. Koltypin , D. Aurbach , (2007). Journal of Power Sources 174: 1241-1250.

[4] G.X. Wang, S. L. B., K. Konstantinov, H.K. Liu, S.X. Dou, J.-H. Ahn (2004). Electrochimica Acta 50: 443-447.

[5] Kiyoshi Kanamura, K. S., Kaoru Dokko (2005). Journal of Power Sources 146: 555-558.

[6] M. Stanley Whittingham, J. C. (2006). Electrochemistry Communications 8: 855-858.

[7] Hal-Bon Gu, E. M. J., Bo Jin, Dae-Kyoo Jun, Kyung-Hee Park, Ki-Won Kim (2008). Journal of Power Sources 178: 801-806.

[8] M. Wohlfahrt-Mehrens, G. A., J. Garche, R. Hemmer, S. Stro¨bele, C. Vogler (2003). Journal of Power Sources 119: 247-251.

[9] Mu-Rong Yang, W.-H. K., She-Huang Wu (2005). Journal of power sources 146: 539-543.

[10] Jou-Hyeon Ahn, J.-K. K., Jae-Won Choi, Ghanshyam S. Chauhan, Gil-Chan Hwang, Jin-Beom Choi, Hyo-Jun Ahn (2008). Electrochimica Acta 53: 8258-8264.

[11] J. Kim, Y.S. Park, B. Veriansyah, J.-D. Kim, Y.-W. Lee (2008) Chemistry of Materials 20: 6301-6303

[12] Tadafumi Adschiri, Y. H., Kuniio Arai (2000). Industrial & Engineering Chemistry Research 39: 4901-4907.

[13] Tadafumi Adschiri, Y. H., Kiwamu Sue and Kunio Arai (2001). Journal of Nanoparticle Research 3: 227-235.

[14] Kunio Arai, K. S., Yukiya Hakuta, Richard L. Smith, Jr., Tadafumi Adschiri (1999). Journal of Chemical & Engineering Data 44: 1422-1426.

[15] Kiyoshi Kanamura, K. D., Shohei Koizumi, Hiroyuki Nakano (2007). Journal of Materials Chemistry 17: 4803-4810.